Dye Sensitized Solar Cells with x% Cu-TiO_2 Photoelectrode Sensitized from Syzygium malaccense

Nurul Fajriah, Elvan Yuniarti, and Sitti Ahmiatri Saptari
Department of Physics, UIN Syarif Hidayatullah Jakarta, Banten, Indonesia 15412

Abstract: Dye-Sensitized Solar Cells (DSSCs) with Cu-doped TiO_2 photoelectrodes sensitized by dye from Jamaica guava leaves (Syzygium malaccense) have been successfully prepared. The DSSCs were constructed using Cu-TiO_2 photoelectrodes synthesized via the doctor blade method, with variations in Cu dopant concentrations of 0%, 1%, and 5%. The sensitizer dye was obtained using the maceration technique, while the electrolyte solution consisted of iodine, and the counter electrode was a carbon layer derived from a candle flame. The components were assembled in a sandwich-like structure. The layers were characterized by X-ray diffraction (XRD) to determine the phase structure and crystal size. XRD analysis of all Cu-TiO_2 layers identified the TiO anatase phase with a tetragonal crystal structure, and the average crystal sizes, calculated using the Williamson-Hall method, were 60.28 nm, 43.32 nm, and 53.32 nm for 0%, 1%, and 5% Cu doping, respectively. UV-Vis spectrophotometry was used to determine the optical properties of the dye, revealing that the Jamaica guava leaf dye absorbs light at wavelengths between 400-700 nm, with a bandgap energy of 1.728 eV. Current-voltage (I-V) characterization was performed to assess the solar cell efficiency. The results indicate that adding Cu dopants to the photoelectrode can enhance the efficiency of the DSSC at specific concentrations, with the highest efficiency of 0.0036% achieved at a 1% Cu doping concentration. This study aims to investigate the effect of different Cu dopant concentrations on the efficiency and performance of DSSCs using natural dye from Syzygium malaccense, specifically comparing DSSCs with no doping, the lowest (1%), and the highest (5%) Cu dopant concentrations.

Keywords: DSSC; Jamaica guava leaf; dopant; Cu-TiO_2

*Corresponding author: elvan.yuniarti@uinjkt.ac.id

http://dx.doi.org/10.12962/j24604682.v20i1.16611
2460-4682

I. INTRODUCTION

Dye-sensitized solar cells (DSSCs) have garnered significant attention as a promising alternative to traditional silicon-based solar cells due to their cost-effectiveness, ease of fabrication, and potential for high efficiency. DSSC is one of the solar cell technologies that convert solar energy, a form of alternative energy, into electrical energy. DSSCs use dyes as light absorbers, which are then transformed into energy in a process similar to photosynthesis in plants. The semiconductor at the photoanode acts as a replacement for CO_2 as an electron acceptor, (I^-/I_3^-) as a substitute for oxygen, water as an electron donor, and oxidation products; the multilayer structure in DSSC is similar to a thylakoid membrane which converts solar energy into electrical energy through dye absorption [1]. DSSCs offer renewable energy solutions with low pollution levels, environmentally friendly production, economical costs, and ease of fabrication. DSSC was first introduced by Michael Grtzel in 1991, using a ruthenium complex as a dye and achieving an efficiency of 13% [2]. However, the limited supply of natural ruthenium complexes and their less environmentally friendly characteristics have led scientists to turn to natural dyes due to their abundant availability and ease of production.

Jamaica guava leaves were chosen as a sensitizer in DSSCs due to their rich pigment content, particularly chlorophyll, which effectively absorbs light and converts it into electricity [3]. Additionally, these leaves contain high levels of bioactive compounds, including carotenoids and terpenes, contributing to their antioxidant properties [3]. The correlation lies in the role of antioxidant properties in stabilizing the dye and reducing recombination rates in DSSCs. Bioactive compounds like carotenoids and terpenes in Jamaica guava leaves have antioxidant properties that help protect the dye molecules from degradation. This stabilization ensures more efficient light absorption and electron transfer.

Additionally, antioxidants reduce charge recombination by neutralizing free radicals that could otherwise recombine with electrons, thus enhancing the overall efficiency of DSSCs by maintaining a steady flow of electrons through the semiconductor [4]. The plant is also known for its adaptability to various soil types and climatic conditions, thriving in humid to subhumid tropical regions, which ensures a reliable supply of raw material for dye extraction [5]. The extraction was performed using the maceration technique, a simple and efficient method [6,7]. Moreover, no previous research has utilized these leaves as a sensitizer, adding novelty to this study. The ease of cultivation and economic considerations in Indonesia also support the choice of Jamaica guava leaves, as these plants are easy to grow and have low costs, reducing the overall production expenses of DSSCs [8].

Besides dye, to increase the efficiency of DSSCs, it is ad-

FIG. 1: Jamaica guava leaf dye

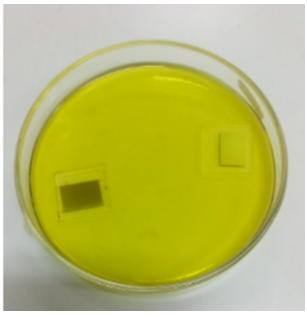

FIG. 2: Immersion of the photoanode in dye

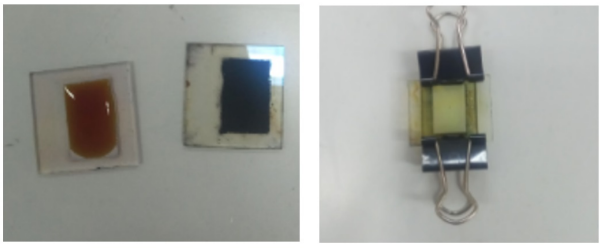

FIG. 3: DSSC assembly

visable to use a semiconductor with a wide surface area, high porosity, and characteristics suitable for the sensitizer used. A frequently chosen semiconductor for photoanode applications is titanium dioxide. Titanium dioxide has good stability and can absorb ultraviolet radiation [9-11]. Furthermore, to improve the performance of solar cells, material engineering on the semiconductor can be conducted to obtain specific characteristics. One of the material engineering strategies is doping the semiconductor with certain metals, such as copper (Cu), to improve the semiconductors electrical properties and overall DSSC efficiency. Previous studies have demonstrated that doping TiO_2 with Cu can enhance the photoelectric properties of the photoanode [12]. For instance, research has shown that low concentrations of Cu can increase the conductivity and reduce the recombination rate in TiO_2 [13]. However, these studies often focus on a narrow range of doping concentrations and do not extensively investigate the effects of higher Cu concentrations on the structural and electronic properties of TiO_2. Furthermore, the techniques used for doping and the methods for characterizing the doped TiO_2 vary widely, leading to inconsistencies in the reported outcomes[14,15].

In the study of DSSCs with Cu doping, the highest efficiencies were achieved at different Cu concentrations across various manuscripts. For instance, in the research conducted by L. B. Patle and A. L. Chaudhari, the highest efficiency of 2.283% was observed with a 1% Cu doping concentration. As the Cu concentration increased to 2% and 3%, the efficiency decreased to 2.058% and 1.673%, respectively [16]. This decline was attributed to the increase in defect density and charge recombination, which negatively impacted the photocurrent density and overall efficiency. Another study by Li Zhou et al. showed that the highest efficiency was achieved with a 1.0% Cu doping concentration, resulting in an efficiency of 6.12% [12]. Beyond this concentration, the efficiency dropped significantly. The improved efficiency at 1.0% Cu was due to enhanced electron injection and reduced charge recombination. However, higher doping levels led to increased impurity concentration and defect sites, which hindered electron transport and reduced efficiency. In research by W.N. Yehya et al., the highest efficiency was observed at a 1.0% Cu doping level with an efficiency of 2.87% [17]. Increasing the Cu concentration to 10% resulted in a drastic decrease in efficiency to 0.12%. The initial improvement at 1.0% Cu was due to better electron injection and charge-transfer efficiency. However, the increased defect sites at higher concentrations caused significant charge recombination, leading to a substantial drop in efficiency.

This study conducted material engineering on the photoanode by applying Cu dopants to TiO_2 with doping fractions of 0%, 1%, and 5%. Based on the results of this study, the optimal doping percentage that most effectively increases the efficiency of the DSSC will be determined.

II. METHODOLOGY

A. Tools and Materials

The tools used in this study included filter paper, a small 120 mL glass bottle, a micropipette, a beaker glass, a glass stirring rod, a petri dish, a magnetic stirrer, a hotplate, spatula, mortar, digital scale, pestle, weighing paper, measuring pipette, dropping pipette, digital multimeter, scotch tape, paperclip, the crucible, furnace, glass bottle, alligator cable, potentiometer, Lux meter, hygrometer, UV-Vis spectrometer, and X-Ray Diffractometer. The materials used were Jamaica guava leaf as a source of dye, distilled water, PEG (Polyethylene Glycol liquid) 400, PVA (Polyvinyl Aldehyde), and 96% methanol as solvents; Indium et al. glass as a substrate; commercial TiO_2 (anatase) and $CuCl_2$ as a semiconductor material on the photoanode; electrolyte made of potassium iodide (KI) and iodine; and candle flame soot as a catalyst at the photoelectrode.

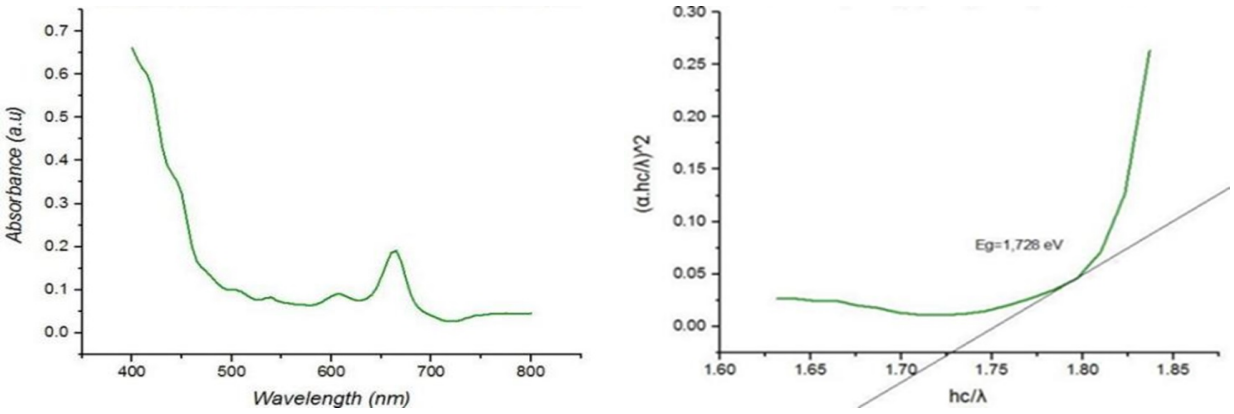

(a) (b)

FIG. 4: (a) UV-vis absorbance spectra, (b) band gap energy of Jamaica guava leaf dye.

B. Preparation of Natural Dye Sensitizers

Chlorophyll was extracted from Jamaica guava leaf by maceration technique, as shown in Fig. 1, which involves soaking 20 g of leaves in methanol solvent in a glass beaker covered with aluminum foil and storing it for 48 hours under impermeable light conditions [18].

C. Preparation of ZnO- TiO_2 Paste

Photoanode preparation includes the manufacture of x% Cu-TiO_2 semiconductor paste, deposition on ITO glass by the doctor blade method, annealing, and immersion in dye. Titanium(IV) oxide (TiO_2) was used as a photoanode material. The TiO_2 paste was prepared by mixing TiO_2 powder (EMSURE, Merck KGaA, Catalog Number: 1.00808.1000) with a small amount of ethanol to form a slurry. This mixture was then ground using a mortar and pestle until a homogeneous paste was obtained. X% Cu-TiO_2 paste is made from a doping and TiO_2 paste mixture. The doping solution is made by mixing 10% solvent of a mixture of distilled water and methanol (10:1) with 0%, 1%, and 5% powder based on the TiO_2 /Cu mole ratio, then stirring with a magnetic stirrer for 10 min. TiO_2 paste is made from a mixture of gel solution made of PVA and hot distilled water, then stirred with a magnetic stirrer at 300 rpm for 30 min at 80°C. After that, add TiO_2 powder and doping solution, then grind it with a mortar for 10 min or until homogeneous. The paste was then coated onto a conductive glass substrate to form a layer with dimensions of 10 mm $\times$ 15 mm by the doctor blade method and then annealed in a furnace at 400°C for 30 min.

D. Preparation of Electrode and Counter Electrode

The counter electrode was prepared by coating another conductive glass substrate with carbon using a method similar to that of Joshi et al. [19]. The curves in Fig. 4 shows that guava dye has light absorption in the visible spectrum range (400-700 nm), while in literature, the chlorophyll pigment is in the 680-700 nm spectrum, which means that the dye solution in this sample succeeded in extracting the chlorophyll substance colour in the guava leaves. This dye has a band gap energy of 1.728 eV, calculated by the Tauc plot method [20]. This value is a low band gap energy, so the energy required for electrons to be excited from the HOMO to the LUMO levels is low, which makes it suitable as a DSSC sensitizer [21]. Black of the mustard oil was prepared as follows: a traditional mustard oil lamp with cotton wicks was used, and the flame was covered with an ITO substrate so that the lamp soot was deposited onto the inner surface of the substrate. The collected lampblack was then applied to the conductive glass substrate to form the carbon layer.

E. DSSC Assembling

The electrolyte solution consisted of potassium iodide (KI) and iodine (I2). Potassium iodide (KI) was sourced from EMSURE, Merck KGaA, Catalog Number: 1.05043.0500, and iodine (I2) from NOVA Laboratorium. Electrolytes are made from a mixture of 8.3 g of KI, 1.26 g of iodine, and 100 mL of PEG, which were stirred using a magnetic stirrer for 30 min, and then stored in bottles coated with aluminum foil. As illustrated in Fig. 3, the DSSC is constructed similarly to a sandwich, with the electrolyte sandwiched between the photoanode and the photoelectrode and offset by 0.5 cm for electrical contact. The two glasses are clamped to maintain the cell structure [22].

F. Characterization

To evaluate the range of the absorbed spectrum and its absorbance value, UV- Vis's characterization was carried out. Current-voltage (I-V) characterization was carried out to ascertain the experimental and theoretical efficiency of DSSC,

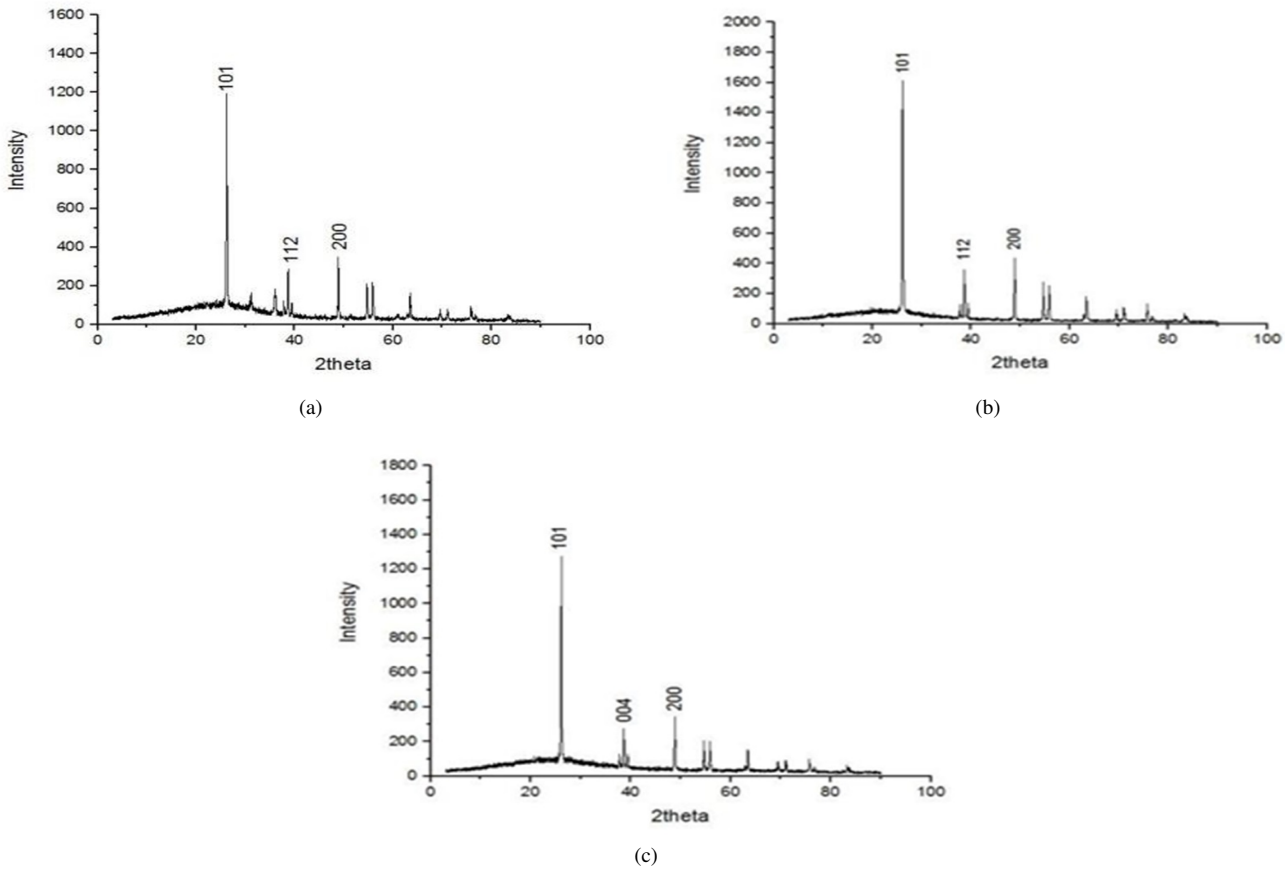

FIG. 5: XRD pattern results at x% Cu-TiO_2; (a) 0% Cu, (b) 1% Cu, and (c) 5% Cu.

and X-ray diffraction characterization was conducted to discover TiO_2 crystal properties. The study of UV-Vis determined the range of the absorbed spectrum and its absorbance value. The TiO_2 crystal properties were discovered by X-ray diffraction investigation. The current-voltage (I-V) analysis was used to ascertain the experimental and theoretical effectiveness of DSSC.

III. RESULTS AND DISCUSSIONS

A. UV - Viss Characterization

Fig. 4 shows that guava dye has light absorption in the visible spectrum range (400-700 nm), while in literature, the chlorophyll pigment is in the 680-700 nm spectrum, which means that the dye solution in this sample succeeded in extracting the chlorophyll substance colour in the guava leaves. This dye has a band gap energy of 1.728 eV, calculated by the Tauc plot method [20]. This value is a low band gap energy, so the energy required for electrons to be excited from the HOMO to the LUMO levels is low, which makes it suitable as a DSSC sensitizer [21].

B. X-Ray Diffraction

Fig. 5 compares the XRD pattern results for samples of 0%, 1%, and 5% Cu-doped TiO_2. These results were compared to COD data for TiO_2 materials with reference codes 96-101-0942 for 0% and 96-101-0943 for 1% and 5%. From the matched phases, an X-ray diffraction pattern analysis was performed to obtain further crystallographic information from the three samples using the Rietveld refinement method. The refinement results for the three samples have reasonably good fitting quality with minimum Rp, wRp, and χ^2 (chi-squared) [23].

The XRD pattern in Fig.5 and the crystallographic data information in Table II show that the element Cu was not identified in the XRD results. These results follow previous studies conducted by Li Zhou et al., which found that adding the element Cu to TiO_2 with doping fractions of 0.7%, 0.9%, 1.0%, 1.2%, and 1.5% did not result in Cu being identified in any XRD results. From these results, it can be inferred that the doping sample has no other peaks or impurities obtained in the XRD pattern, and no CuO element is formed in the x% Cu- sample, indicating that the Cu dopants have entered the TiO_2 crystal lattice [18]. Additionally, the absence of other compound peaks in the XRD pattern indicates that the annealing process was successful. The heat treatment after drying

TABLE I: XRD characterization data for the three highest peaks in each doping fraction

TiO_2 phase	HKL	Peak 2θ	FWHM(°)
	101	26.20415	0.17961
0% Cu-TiO_2	112	38.67441	0.20955
	200	48.89638	0.23355
	101	26.11616	0.21417
1% Cu-TiO_2	112	38.60587	0.21482
	200	48.83359	0.2469
	101	26.13264	0.19126
5% Cu-TiO_2	4	38.60896	0.22135
	200	48,82914	0.23991

the x% Cu-TiO_2 layer is to make the material active for the photocatalytic reaction and to ensure uniformity in the anatase phase in TiO_2, which in previous studies was formed at around 400°C [19].

From the results already mentioned, the average crystal size at 1% Cu-TiO_2, 43.32 nm, is smaller than the average crystal size of 0% and 5% Cu-TiO_2. The smaller crystal size at 1% Cu doping can be attributed to the substitutional doping effect, where Cu^{2+} ions replace Ti^{4+} ions, causing lattice distortion and strain, limiting crystal growth and producing finer crystals. At 0% Cu doping, the absence of additional strain allows for more considerable crystal growth. In contrast, at 5% Cu doping, the excessive number of Cu^{2+} ions introduces more significant lattice strain and defects, which initially reduce the crystal size but also disrupt the crystal structure. This disruption can lead to the resumption of crystal growth in certain regions, resulting in a larger average crystal size compared to 1% doping but still smaller than the undoped sample.

Based on the X-ray diffraction pattern data in Table I, each peak at 2θ has different FWHM, hkl, and crystal sizes. The crystal size can be calculated using the Williamson-Hall method [24]. From the results of the crystal size calculation using the Williamson-Hall method, it was found that the strain factor caused the width of the diffraction peaks to increase, resulting in a decrease in crystal size. The reduction in crystal size is due to the dopant element Cu entering the TiO_2 crystal lattice substitutionally, given the slight difference in ionic radii between Cu^{2+} (87 pm) and Ti^{4+} (74.5 pm). A decrease in lattice parameters accompanies the entry of Cu^{2+} ions into Ti sites due to the high electron affinity of Cu^{2+}, which donates 2e to Ti^{4+} [25].

Table II shows the results of adding 1% and 5% Cu doping without changing the crystal structure of TiO_2. These results show that the three samples have an anatase phase with a tetragonal crystal structure. This is by previous research.

Table III shows the results that the average crystal size at 1% Cu-TiO_2, 43.32 nm, is smaller than the average crystal size of 0% and 5% Cu-TiO_2. The smaller crystal size at 1% Cu doping can be attributed to the substitutional doping effect, where Cu^{2+} ions replace Ti^{4+} ions, causing lattice distortion and strain, limiting crystal growth and producing finer crystals. At 0% Cu doping, the absence of additional strain allows for more considerable crystal growth. In contrast, at 5% Cu doping, the excessive number of Cu ions introduces more significant lattice strain and defects, which initially reduce the crystal size but also disrupt the crystal structure. This disruption can lead to the resumption of crystal growth in certain regions, resulting in a larger average crystal size compared to 1% doping but still smaller than the undoped sample.

From these results, the average crystal size of 1% Cu-TiO_2 (43.32 nm) is smaller than the average crystal size of 0% and 5% Cu-TiO_2. A smaller crystal size results in a larger surface area, which can adsorb more dye [21]. Additionally, the cause of the low DSSC efficiency of 5% Cu-doped TiO compared to 1% Cu-doped TiO_2 is thought to be due to the large number of electrons trapped in the doped metal. This hypothesis is supported by the XRD results, which show increased strain and defects at higher doping concentrations. These defects act as recombination centers, trapping electrons and reducing overall efficiency. Therefore, while Cu doping can enhance efficiency by improving light absorption and electron transport, there is an optimal doping concentration (1%) beyond which the introduction of defects outweighs the benefits [19, 23, 24].

TABLE II: Crystal structure data TiO_2 anatase phase

Structure Parameter	0% Cu-TiO_2	0% Cu-TiO_2	0% Cu-TiO_2
Room group	I 41/amd	I 41/amd	I 41/amd
Crystal Structure	Tetragonal	Tetragonal	Tetragonal
Corner	= 90	= 90	= 90
Grid parameter:			
a($\AA$)	3.78432	3.782533	3.784024
b($\AA$)	3.78432	3.782533	3.784024
c($\AA$)	9.512178	9.50675	9.510414
Volume ($\AA^3$)	136.225	136,018	136,178
Density (gr/cm^3)	3.896	13,889	11,635
R_{wp} (%)	14.94	14.84	12.35
R_p (%)	11.7	11.5	9.59
χ^2	1.176	1.039	0.8221
Bond length ($\AA^3$)	1,874	1,874	1,874
Bond Angle (°)	43.2985	43.2985	43.2985

TABLE III: Average crystal of Cu-TiO_2 samples with x% variations

	Doping fraction X% Cu-TiO_2		
	0%	1%	5%
Crystal Size			
average (nm)	60.28	43.32	53.32
Strains	0.09	0.03	0.08

TABLE IV: Table of DSSC Efficiency x% Cu-TiO_2

X% Cu-TiO_2	Lux	VOC (mV)	ISC (μA)	Efficiency ($\times 10^4$ %) Theoretical	Experiment
0%	79730	55.6	0.57	126,80	105,90
1%	14120	40.7	5.25	104,44	36,24
5%	31690	192.3	5.34	19,33	13,19

C. Current and Voltage Characterization

Table IV is obtained from the calculations of the equations derived from previous research. From the results in Table IV, there are differences in efficiency values between DSSCs with 0%, 1%, and 5% Cu-doped TiO_2 photoanodes. The DSSC with 1% Cu dopant has higher efficiency than the DSSC without Cu dopant. This result aligns with the theory of the effect of adding dopants, which states that when a semiconductor is doped with an element having excess electrons, donor energy levels are introduced, thereby reducing the energy required for electrons to be excited from the valence band to the conduction band, also known as the band gap energy [26]. However, the lower efficiency of the DSSC with 5% Cu-doped TiO_2 compared to 1% Cu-doped TiO_2 is likely due to the large number of electrons trapped in the doped metal. The metal dopant ions act as recombination centers, making electron transfer to the interface more difficult, thereby significantly reducing photocatalytic activity [19, 23, 24]. Thus, there is an optimum concentration of metal ion dopants where photocatalytic activity is not hindered.

IV. CONCLUSION

This study concludes that x% Cu-TiO_2 photoelectrode sensitized from Jamaica guava leaf dye (TiO_2) has been successfully fabricated. The X-ray diffraction characterization results show that the TiO_2 anatase phase compound with a tetragonal crystal structure and average crystal size calculated using the Williamson-Hall method for 0%, 1%, and 5% Cu doping fractions are 60.28 nm, 43.32 nm, and 53.32 nm, respectively. UV-Vis characterization results indicate that Jamaica guava leaf dye has light absorption at a wavelength between 400-700 nm with a band gap energy of 1.728 eV. Current-voltage (I-V) characterization shows that adding Cu dopants to the photoelectrode can increase the efficiency of DSSC at a specific concentration, with the highest efficiency achieved being 0.0036% at 1% Cu doping concentration.

Acknowledgments

Thank you to PUSLITPEN UIN Syarif Hidayatullah Jakarta. for funding this research. We also extend our gratitude to PLT UIN Syarif Hidayatullah Jakarta for their support this research.

[1] S. N. Karthick, *et al.*, "Dye-sensitized solar cells: History, components, configuration, and working principle," Interfacial Engineering of Functional Materials for Dye-Sensitized Solar Cells, pp. 116, 2019, doi: 10.1002/9781119557401.ch1.

[2] M. Grtzel, "Perspectives for dye-sensitized nanocrystalline solar cells," Progress in Photovoltaics: Research and Applications, vol. 8, no. 1, pp. 171185, 2000, doi: 10.1002/(SICI)1099-159X(200001/02)8:1<171::AID-PIP300>3.0.CO;2-U.

[3] A.G. Batista, *et al.*, "Red-jambo (Syzygium malaccense): Bioactive compounds in fruits and leaves," LWT - Food Science and Technology, vol. 76, pp. 284291, 2017, doi: 10.1016/j.lwt.2016.05.013.

[4] M. Yasir, "Bioactive Compounds of Avocado" (Persea americana Mill.), 2019, doi: 10.1007/978-3-030-06120-3-12-1.

[5] X. D. Crystallography et al., "Trees for life in Oceania," Foods, vol. 9, no. 1, p. 278, 2018.

[6] Hasby, Nurhafidhah, G. Pamungkas, and S. A. Akbar, "Dye-sensitized solar cells properties from natural dye as light-reaping materials extracted from gayo arabica coffee husks," Rasayan Journal of Chemistry, vol. 13, no. 1, pp. 3843, 2020, doi: 10.31788/RJC.2020.1315576.

[7] I. N. Setiawan, *et al.*, "Natural dyes extracted from bioactive components of fruit waste for dye-sensitized solar cell," International Journal of Engineering Research & Technology, vol. 13, no. 9, pp. 24982504, 2020, doi: 10.37624/ijert/13.9.2020.2498-2504.

[8] M. Jawal, "Menggapai laba dari budidaya jambu bol (Syzygium malaccense (L) Merr & Perry)", July 2022.

[9] M. Kashif, *et al.*, "An experimental and DFT study on novel dyes incorporated with natural dyes on titanium dioxide (TiO_2) towards solar cell application," Applied Physics A: Materials Science and Processing, vol. 126, no. 9, pp. 113, 2020, doi: 10.1007/s00339-020-03896-6.

[10] W. Y. Huang and T. L. Hsieh, "Dyes amount and light scattering influence on the photocurrent enhancement of titanium dioxide hierarchically structured photoanodes for dye-sensitized solar cells," Coatings, vol. 10, no. 1, 2020, doi: 10.3390/coatings10010013.

[11] M. K. Son and H. Seo, "Effect of ultraviolet radiation on the long-term stability of dye-sensitized solar cells," Electronic Materials Letters, vol. 16, no. 6, pp. 556563, 2020, doi: 10.1007/s13391-020-00249-6.

[12] L. Zhou , *et al.*, "Improved performance of dye sensitized solar cells using Cu-doped TiO_2 as photoanode materials: Band edge movement study by spectroelectrochemistry," Chemical Physics, vol. 475, pp. 18, 2016, doi: 10.1016/j.chemphys.2016.05.018.

[13] K. Sahu, M. Dhonde, and V. V. S. Murty, "Microwave-assisted hydrothermal synthesis of Cu-doped TiO_2 nanoparticles for efficient dye-sensitized solar cell with improved open-circuit voltage," International Journal of Energy Research, vol. 45, no. 4, pp. 54235432, 2021, doi: 10.1002/er.6169.

[14] M. Ikram, *et al.*, "Dye degradation performance, bactericidal behavior and molecular docking analysis of Cu-doped

TiO_2 nanoparticles," RSC Advances, vol. 10, no. 41, pp. 2421524233, 2020, doi: 10.1039/d0ra04851h.

[15] D. Dahlan, *et al.*, "Synthesis of two-dimensional nanowall of Cu-doped TiO_2 and its application as photoanode in DSSCs," Physica E: Low-Dimensional Systems and Nanostructures, vol. 91, no. May, pp. 185189, 2017, doi: 10.1016/j.physe.2017.05.003.

[16] L. B. Patle and A. L. Chaudhari, "Performance of DSSC with Cu doped TiO_2 electrode prepared by dip coating technique," International Journal of Scientific & Engineering Research, vol. 7, no. 8, pp. 10041009, 2016. [Online]. Available: http://www.ijser.org

[17] S. Chahid, D. M. de los Santos, and R. Alcntara, "The effect of Cu-doped TiO_2 photoanode on photovoltaic performance of dye-sensitized solar cells," ACM International Conference Proceeding Series, 2018, doi: 10.1145/3286606.3286854.

[18] I. Kurniawati, Maftuch, and A. M. Hariati, "Penentuan pelarut dan lama ekstraksi terbaik pada teknik maserasi Gracilaria sp. serta pengaruhnya terhadap kadar air dan rendemen," Samakia: Jurnal Ilmu Perikanan, vol. 7, no. 2, pp. 7277, 2016. [Online]. Available: http://www.samakia.aperiki.ac.id/index.php/JSAPI/article/view/106

[19] P. Joshi, U. Lawaju, and B. B. K., "Composite of lampblack and printer toner powder as a low-cost counter electrode material for dye-sensitized solar cells," Bibechana, vol. 17, pp. 5866, 2020, doi: 10.3126/bibechana.v17i0.25598.

[20] A. Z. Johannes, R. K. Pingak, and M. Bukit, "Tauc Plot Software: Calculating energy gap values of organic materials based on Ultraviolet-Visible absorbance spectrum," IOP Conference Series: Materials Science and Engineering, vol. 823, no. 1, 2020, doi: 10.1088/1757-899X/823/1/012030.

[21] J. Bredas, "Materials Horizons," pp. 1719, 2014, doi: 10.1039/c3mh00098b.

[22] M. C. Misbachudin, F. S. Rondonuwu, and A. Sutresno, "Pengaruh pH larutan antosianin strawberry dalam prototipe dye sensitized solar cell (DSSC)," Jurnal Fisika dan Aplikasinya, vol. 10, no. 2, p. 57, 2014, doi: 10.12962/j24604682.v10i2.794.

[23] K. Moto, L. Setiarini, and Z. Abubakar, "Analisis komposisi fasa dengan metode Rietveld dan pengaruhnya terhadap kekerasan nanokomposit Ti-Si-N," Makara Teknologi Seri, vol. 7, no. 1, pp. 1014, 2010, doi: 10.7454/mst.v7i1.143.

[24] S. K. K. Shaat, *et al.*,"Structural parameters of hydrothermally synthesized ZnO nanostructure and their based solar cells," Nano-Structures & Nano-Objects, vol. 23, p. 100515, 2020, doi: 10.1016/j.nanoso.2020.100515.

[25] A. Tamarani, R. Zainul, and I. Dewata, "Preparation and characterization of XRD nano Cu-TiO_2 using sol-gel method," Journal of Physics: Conference Series, vol. 1185, no. 1, 2019, doi: 10.1088/1742-6596/1185/1/012020.

[26] A. N. Ossai, *et al.*, "Enhanced photovoltaic performance of dye-sensitized solar cells-based Carica papaya leaf and black cherry fruit co-sensitizers," Chemical Physics Impact, vol. 2, no. April, p. 100024, 2021, doi: 10.1016/j.chphi.2021.100024.